DOI: 10.1002/chem.200701038

Preferred Functionalization of Metallic and Small-Diameter Single-Walled Carbon Nanotubes by Nucleophilic Addition of Organolithium and -Magnesium Compounds Followed by Reoxidation

David Wunderlich, Frank Hauke, and Andreas Hirsch*[a]

Abstract: Covalent sidewall addition to single-walled nanotubes (SWNTs) of a series of organolithium and organomagnesium compounds (*n*BuLi, *t*BuLi, EtLi, *n*HexLi, *n*BuMgCl, *t*BuMgCl) followed by reoxidation is reported. The functionalized R_n-SWNTs were characterized by Raman and NIR emission spectroscopy. The reaction of SWNTs with organolithium and magnesium compounds exhibits pronounced selectivity: in general, metallic tubes are more reactive than semiconducting ones. The reactivity of SWNTs toward the addition of organometallic compounds is inversely proportional to the diameter of the tubes. This was determined simultaneously and independently for both metallic and semiconducting SWNTs. The reactivity also depends on the steric demands of the addend. Binding of the bulky *t*-butyl addend is less favorable than addition of primary alkyl groups. Significantly, although *t*BuLi is less reactive than, for example, *n*BuLi, it is less selective toward the preferred reaction with metallic tubes. This unexpected behavior is explained by fast electron transfer to the metallic SWNTs having low-lying electronic states close to the Fermi level, a competitive initial process. The NIR emission of weakly functionalized semiconducting SWNTs, also reported for the first time, implies interesting applications of functionalized tubes as novel fluorescent reporter molecules.

Keywords: carbon · electron transfer · nanotubes · nucleophilic addition · reactivity · selectivity

Introduction

Addition reactions to the sidewalls of single-walled carbon nanotubes (SWNTs)[1] are among the most important functionalization methods in the field of new carbon allotrope chemistry.[2] These transformations are accompanied by the formation of sidewall sp^3 C atoms carrying the covalently bound addends. The major interest in sidewall functionalization of SWNTs is driven by opportunities such as: 1) to increase the solubility and processibility; 2) to combine their properties with those of other classes of compounds; 3) to increase the functionality; and last but not least 4) to study the intrinsic chemical properties of SWNTs. The most interesting chemical properties with respect to sidewall functionalization are 1) the reactivity and 2) the selectivity of individual exfoliated tubes toward either the direct binding of addends or the binding of addends accompanied by preceding electron-transfer reactions.

The available experimental and theoretical work on sidewall additions reveals clearly that the reactivity of SWNTs toward addition reactions is considerably lower than that of classical molecules involving a conjugated π system.[2,3] Only very reactive addends undergo addition reactions with the tubes. Also, the related fullerenes such as C_{60} are more reactive than SWNTs because the "sp^2 C atoms" of the fullerene core are considerably more pyramidalized, even when the diameter of the tubes is as small as that of C_{60}, for example.[3,4] Whereas C_{60} easily undergoes [4+2] cycloadditions with mild dienes[5] such as cyclopentadiene, only a few examples of reactions of very reactive dienes with SWNTs have been reported.[6]

As prepared, SWNT samples consist of a mixture of tubes with different diameters and helicities. Diameter-dependent selectivity of addition reactions is expected.[3,4] In the case of direct covalent binding of an addend, tubes with smaller diameter should be attacked preferentially. Their C atoms exhibit a higher degree of pyramidalization and consequently store more strain energy. Experimentally, the preferred burning,[7] etching,[8] or ozonation[9] of smaller-diameter

[a] Dipl.-Chem D. Wunderlich, Dr. F. Hauke, Prof. Dr. A. Hirsch
Institut für Organische Chemie and Zentralinstitut für
Neue Materialien und Prozesstechnik (ZMP)
Universität Erlangen–Nürnberg, 91052 Erlangen (Germany)
Fax: (+49) 9131-852-253
E-mail: hirsch@chemie.uni-erlangen.de

tubes has been observed, but no detailed experimental investigation of the dependence of selectivity on tube diameter in the addition of organic addends has been reported yet except in the addition of diazonium salts, where it was found, however, that for semiconducting SWNTs the reactivity increases with increasing diameter.[10] Conceptually, further selectivity mechanisms are associated with the helicity or the metal versus the semiconductor behavior of SWNTs. Selectivity based on differing helicities has so far been reported in theoretical contributions only,[4c] but the first experimental evidence for higher reactivity of metallic versus semiconducting tubes has already been provided.[10–12]

We have recently reported a clean method for the synthesis of *t*-butylated SWNTs by a nucleophilic alkylation followed by reoxidation.[12] Similarly to Billups' reductive alkylation in liquid ammonia,[13] this functionalization method has the advantage that the very soluble, negatively charged intermediates are exfoliated, owing to electrostatic repulsion. Consequently tubes can be addressed chemically as individuals and are not agglomerated in bundles. Significantly, we have received the first evidence for a preferred alkylation of metallic over semiconducting nanotubes.[12] This preference can be explained by the availability of accessible electronic states close to the Fermi level, which leads to a stabilization of transition states during the covalent attachment of a nucleophilic addend (Figure 1).[12] Along the same

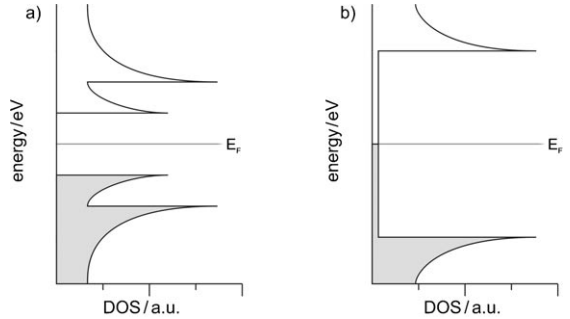

Figure 1. Schematic representation of the density of electronic states (DOS) for a) a semiconducting and b) a metallic nanotube.

lines, the selectivity can also be explained by a traditional chemical concept reported by Joselevich, stating that the metallic species are less aromatic and have a smaller HOMO–LUMO gap.[14]

We recognized that this reaction sequence offers exciting opportunities for the systematic investigation of the selectivity principles of addition reactions to SWNT sidewalls. We now report on some fundamental aspects of SWNT chemistry based on Raman and fluorescence spectroscopic characterization of SWNT derivatives obtained from the reaction with a series of organolithium and organomagnesium compounds followed by reoxidation. In particular, we show for the first time that: 1) for a whole series of organometallic compounds metallic SWNTs are more reactive than semiconducting ones; 2) the reactivity of SWNTs toward the addition of organometallic compounds is inversely proportional to the diameter; 3) the dependence on diameter of selectivity holds for both metallic- and semiconducting SWNTs, simultaneously and independently; 4) the selectivity of the addition to metallic tubes versus semiconducting tubes is not correlated inversely with the reactivity of organometallic compounds toward sterically nonhindered substrates; and 5) weakly functionalized semiconducting tubes still fluoresce in the near infrared (NIR).

Results and Discussion

Commercially available purified HiPco® SWNTs[15] (CNI) were used as starting materials. They were further purified by sonication and boiling in concentrated hydrochloric acid to remove iron catalyst particles. Before treatment with an organometallic reagent, the tubes were dispersed in anhydrous cyclohexane in an ultrasonic bath under an inert gas atmosphere to disintegrate larger particles and disperse the bundles. To this dispersion, which reagglomerates easily when the sonication is stopped, a fivefold excess of a solution of *n*-butyllithium, *t*-butyllithium, ethyllithium, *n*-hexyllithium, *n*-butylmagnesium chloride, or *t*-butylmagnesium chloride was added slowly (Scheme 1). The reaction mixture was stirred for 30 min and subsequently sonicated for 30 min to facilitate the reaction with the organometallic

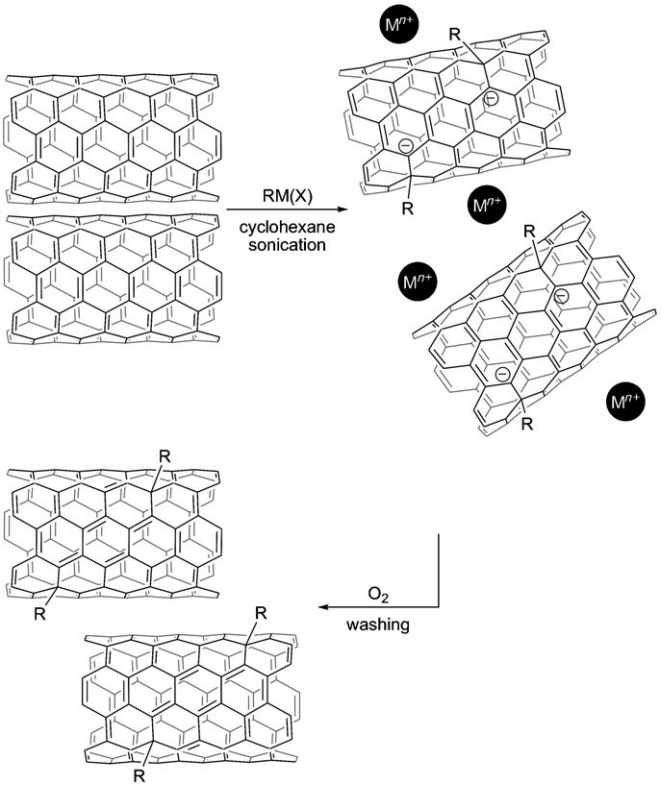

Scheme 1. Alkylation of SWNTs by RM(X) followed by reoxidation. R = *n*Bu, *t*Bu, Et, or *n*Hex; M = Li or Mg; X = Cl (for M = Mg).

compounds. During this process a very stable homogeneous dispersion was formed. As we have shown previously, the stability of the black dispersions of dissolved tubes is a result of the electrostatic repulsion of the intermediates R_n-SWNT^{n-} that causes exfoliation of the bundles (Scheme 1).[12] The intermediates R_n-SWNT^{n-} are formed by addition of the addends R to the sidewalls of the tubes, accompanied by the transfer of one electron per R. This reaction is also well known as the initial step of the hydroalkylation and arylation of fullerenes such as C_{60} and C_{70}.[5] After the sonication step the reaction mixture was stirred for another 20 h. Subsequently, the intermediates R_n-SWNT^{n-} were oxidized to give the reaction products R_n-SWNT by bubbling oxygen through the solution for 30 min (Scheme 1).

During this procedure the tubes are precipitated, owing to aggregation caused by the removal of the negative charge. The corresponding reaction products are denoted as $R_n(M)$-SWNT with *M* indicating the metal of the organometallic reagent (Li or Mg). We have replaced the carcinogenic benzene in our previous report on the *t*-butylation of SWNTs[12] by cyclohexane. SWNT alkylation with *n*BuLi and *t*BuLi in a variety of solvents showed, for example, that THF[16] is not suitable because the dispersion of the SWNTs in the presence of the organometallic reagent obtained by sonication was not stable. Most importantly, Raman spectroscopy revealed that almost no functionalization of the carbon nanotubes took place. Comparative results were obtained when a benzene/THF mixture (1:1) was used as solvent. Significantly, cyclohexane proved to be as good as benzene and was therefore used to replace benzene in this study. The comparison of reactions with *n*BuMgCl and *t*BuMgCl at RT and 0 °C revealed no significant difference. The alkylated derivates R_n-SWNT are more soluble in organic solvents such as 1,2-dichloroethane than the unmodified tubes, but less soluble in water in the presence of sodium dodecylbenzenesulfonate (SDBS) as surfactant. TGA-MS analysis revealed the presence of covalently bound addends by the unequivocal determination of their molecular mass after thermal cleavage in the 160–440 °C range.

Raman spectroscopy is one of the most powerful methods for investigating covalent sidewall functionalization.[17] Covalent binding of addends characteristically affects the intensity ratio of the SWNT Raman bands. The most noticeable change is an increase in the intensity of the D band ($\approx$1250–1450 cm^{-1}), which arises from the generation of sp^3 C atoms as defects in the sidewalls, relative to those of the radial breathing modes (RBMs) ($\approx$100–300 cm^{-1}) and the G band ($\approx$1500–1600 cm^{-1}). The intensity ratio between the D band and the G band is therefore taken as a parameter for the extent of functionalization.[2,18] However, highly functionalized SWNTs do normally exhibit reduced intensities of the RBMs and the G band in comparison to the unmodified tubes.[19] For this behavior two possible explanations can be considered. Firstly, the covalent modification disrupts the electronic band structure, thus reducing the resonance enhancement of the Raman process significantly. The same phenomenon also reduces the intensity of the D band at very high degrees of functionalization.[11a] Second, the decrease in intensity is related to functionalization-induced changes in the overall symmetry and bonding structure of the tubes.[18] By using the area ratio of the D peak to the G peak (A_D/A_G) as a parameter for the extent of the functionalization, we normalize all Raman spectra to the intensity of the G band. Raman spectroscopy is a resonant process: that is, Raman signals of particular carbon nanotubes are greatly enhanced if either the incoming laser energy or the scattered radiation matches an allowed electronic transition of the tube (single resonance). Therefore, it is possible to address different kinds of SWNTs with different excitation wavelengths. The assignment of tubes that are resonant for a given wavelength has been investigated carefully and systematically and can be taken from the "Kataura plots."[11b,20] In our experiments we used two different excitation wavelengths: 532 nm is predominantly resonant for metallic nanotubes, whereas 780 nm is predominantly resonant for semiconducting tubes.[11b] In both cases characteristic changes of the intensities of the D bands and RBMs can be observed after covalent sidewall functionalization. The D band also shows dispersive behavior (the peak frequency increases with increasing laser excitation energy). For the Raman measurements R_n-SWNT samples were prepared as bucky papers.

The G bands obtained with 532 nm excitation exhibit a pronounced asymmetry at the low-frequency side, which is attributed to a Breit–Wigner–Fano (BWF) resonance of metallic nanotubes (Figure 2, right). At 780 nm excitation

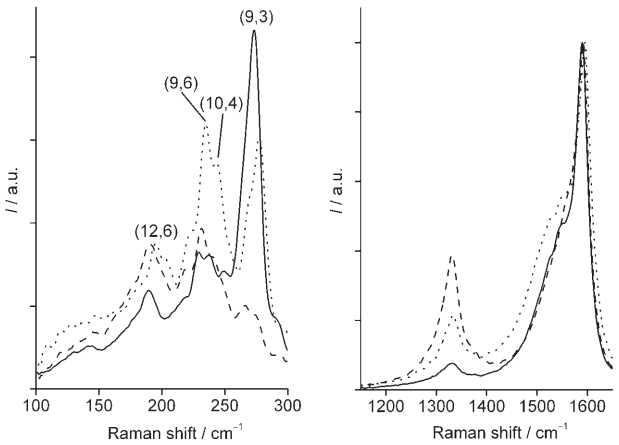

Figure 2. Raman spectra (532 nm excitation) of pristine SWNTs (solid line), $n\text{Bu}_n(Li)$-SWNTs (broken line), and $t\text{Bu}_n(Li)$-SWNTs (dotted line).

the G band splits into a higher-frequency (G^+) and a lower-frequency (G^-) component; both exhibit a symmetric line shape and are attributed to semiconducting nanotubes (Figure 3, right).[21]

The Raman spectra of the pristine material, $n\text{Bu}_n(Li)$-SWNTs, and $t\text{Bu}_n(Li)$-SWNTs excited at 532 and 780 nm are shown in Figures 2 and 3, respectively. It is clear from the

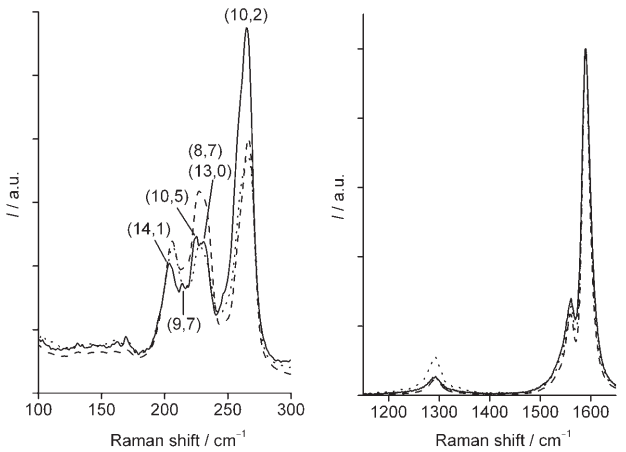

Figure 3. Raman spectra (780 nm excitation) of pristine SWNTs (solid line), *n*Bu$_n$(*Li*)-SWNTs (broken line), and *t*Bu$_n$(*Li*)-SWNTs (dotted line).

Table 1. Comparison of the Raman (A_D/A_G) ratios of the samples for two different excitation wavelengths. Also given are qualitative indications of the reactivity and the selectivity of the relevant organometallic reagent toward alkylation of SWNTs.

Sample	Raman, 532 nm		Raman, 780 nm	
	A_D/A_G[a]	Reactivity	A_D/A_G[a]	Reactivity
*n*Bu$_n$(*Li*)-SWNTs[b]	5.8	high	1.5	intermediate
*t*Bu$_n$(*Li*)-SWNTs[c]	1.9	intermediate	1.7	intermediate
*n*Bu$_n$(*Mg*)-SWNTs[d]	2.4	high	1.3	low
*t*Bu$_n$(*Mg*)-SWNTs[e]	1.2	low	1.0	low

[a] Values are the ratios A_D/A_G relative to A_{D0}/A_{G0} of the pristine SWNTs. [b–e] Average values of [b] 5, [c] 11, [d] 5, and [e] 4 different experiments.

average values for the ratio of A_D/A_G to A_{D0}/A_{G0} of the pristine SWNTs (Table 1) that the intensities of the D bands increase considerably after functionalization, especially for excitation at 532 nm, where the metallic tubes are addressed. Significantly, *n*-butyllithium is much more reactive to metallic tubes than *t*-butyllithium. Yet *t*-butyllithium produces a higher degree of functionalization in the semiconducting tubes than *n*-butyllithium. For *n*Bu$_n$(*Li*)-SWNT the A_D/A_G ratio at 532 nm is almost four times that at 780 nm. The conclusion is that *n*-butyllithium *is* more reactive than *t*-butyllithium but, most interestingly, it is more selective toward metallic tubes. This behavior is counterintuitive at first glance. Our interpretation is given below.

The RBM part of the Raman spectra taken at 532 nm excitation reveals four predominant metallic M_{11} transitions at 190, 229, 239, and 273 cm^{-1}, which are typical for the HiPco nanotubes (Figures 2 and 3, left). The calculated diameters of the corresponding tubes using the relationship $\omega_{RBM} = Ad_t^{-1} + B$ ($A = 223.5$ nm cm^{-1}, $B = 12.5$ cm^{-1})[22] are (from left to right) 1.26, 1.04, 0.99, and 0.86 nm. By using the modified Kataura plot[11b] it is possible to assign the peaks to the (12,6), (9,6), (10,4), and (9,3) chirality indices. In the regime of the metallic tubes, the intensity changes in the RBM region at 532 nm excitation caused by the alkylation are correlated inversely with the changes in the D-band intensities (Figure 2). Most significantly, the decreases in the intensities of the bands attributed to the small-diameter tubes such as the (9,3) band at 273 cm^{-1} are considerably more pronounced with increasing D-band intensity than those of the higher-diameter SWNTs such as the (12,6) tube (Figure 2, left). For *t*Bu$_n$(*Li*)-SWNT the RBM intensities of tubes with intermediate diameters, for example, (9,6) and (10,4), are almost equal to the intensity of the (9,3) band. In the highly functionalized *n*Bu$_n$(*Li*)-SWNT the band of the (9,3) mode has almost disappeared. In contrast, the intensity of the RBM of the highest-diameter (12,6) tube is almost equal to those of the (10,6) and (9,6) tubes. The conclusion from these results is that there is pronounced selectivity associated with the alkylation of metallic SWNTs: the reactivity of metallic tubes is correlated inversely with the diameter. The decrease in RBM intensity in functionalized R$_n$-SWNTs is a result of the reduction of symmetry caused by the binding of addends. Conceptually, an ensemble of functionalized tubes with a given (*m,n*) helicity is expected to be completely desymmetrized, since even for the ideal case in which every tube contains the same number of addends R a myriad of regioisomers will be formed.

At 780 nm excitation, five S_{22} bands for semiconducting tubes at 205, 215, 225, 230, and 265 cm^{-1} (Figure 3, left) can be seen. From the Kataura plot these can be attributed to the (14,1), (9,7), (10,5), (8,7) and/or (13,0), and (10,2) tubes, respectively. The corresponding diameters are 1.15, 1.10, 1.05, 1.03, and 0.88 nm. In the samples of functionalized *n*Bu$_n$(*Li*)-SWNTs and *t*Bu$_n$(*Li*)-SWNTs the (9,7), (10,5), and (8,7)/(13,0) modes are not resolved. The most pronounced decrease in intensity is observed for the (10,2) tubes of the smallest diameter. However, compared to the metallic (9,3) tubes addressed at 532 nm excitation this decrease is less prominent. The conclusion from this set of experiments is again that the reactivity of semiconducting tubes is correlated inversely with the diameter. Results obtained for the functionalization of SWNTs with ethyllithium and *n*-hexyllithium are comparable to those of the *n*-butyllithium reaction: there is pronounced selectivity of 1) metallic tube functionalization and 2) small-diameter tube functionalization for both metallic and semiconducting tubes.

To investigate further the influence of the nucleophilicity of the functionalization reagent, we also prepared the alkylated *n*Bu$_n$(*Mg*)-SWNT and *t*Bu$_n$(*Mg*)-SWNT tubes by alkylating the SWNTs with the less reactive Grignard reagents *n*BuMgCl and *t*BuMgCl (Scheme 1). Comparison of the D-band and RBM intensities of the Raman spectra of the pristine starting material, *n*Bu$_n$(*Mg*)-SWNT, and *t*Bu$_n$(*Mg*)-SWNT excited at 532 nm and 780 nm (Figures 4 and 5) and the A_D/A_G ratios (Table 1) confirms the expectation that *n*BuMgCl is a much weaker alkylation agent than *n*BuLi. Most significantly it reacts very selectively with the small-diameter metallic SWNTs. In the semiconducting regime addressed by 780 nm excitation the intensity changes of the D band and the RBMs are negligibly low, leading to the conclusion that *n*BuMgCl is not very reactive to semiconducting

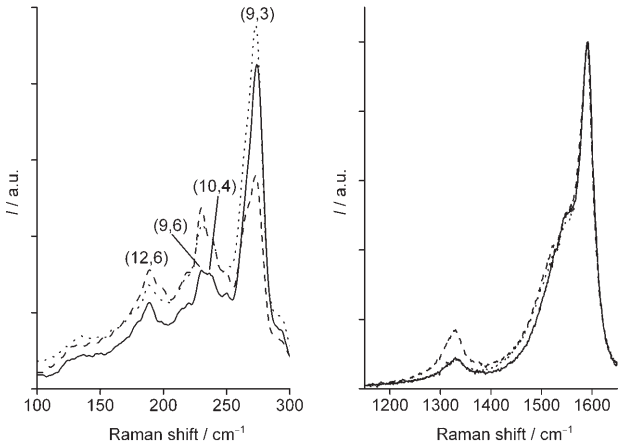

Figure 4. Raman spectra (532 nm excitation) of pristine SWNTs (solid line), $n\mathrm{Bu}_n(Mg)$-SWNTs (broken line), and $t\mathrm{Bu}_n(Mg)$-SWNTs (dotted line).

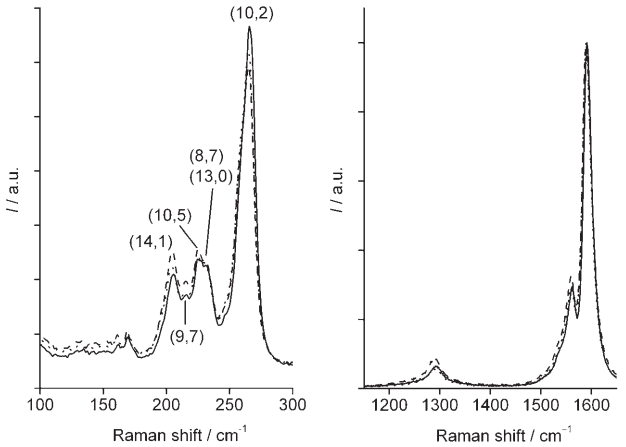

Figure 5. Raman spectra (780 nm excitation) of pristine SWNTs (solid line), $n\mathrm{Bu}_n(Mg)$-SWNTs (broken line) and $t\mathrm{Bu}_n(Mg)$-SWNTs (dotted line).

tubes. The same analysis of the Raman spectra of $t\mathrm{Bu}_n(Mg)$-SWNTs reveals that *t*BuMgCl is very unreactive to both metallic and semiconducting SWNTs.

The reactivity and selectivity profile of the organometallic reagents toward alkylation of SWNTs is indicated qualitatively as high, intermediate, or low in Table 1. In general, the organolithium compounds are more reactive than the Grignard compounds, as expected. *n*BuLi is more reactive than *t*BuLi. However, *n*BuLi is more selective toward metallic tubes. Among the Grignard compounds, *t*BuMgCl is less reactive than *n*BuMgCl. Almost no indication of a sidewall functionalization can be deduced from Raman spectroscopy, in contrast to the more sensitive fluorescence spectroscopy (see below). The reactivity of a tube is correlated inversely with its diameter. The lower reactivity of the *t*Bu compounds than the *n*Bu compounds can be explained by the steric bulk of the *t*Bu group, which disfavors covalent bond formation. The steric hindrance of the *t*Bu groups has already been recognized in fullerene chemistry. NMR spectroscopic investigations of *t*Bu-C_{60}^- prepared by the analogous reaction of *t*BuLi with C_{60} revealed a hindered rotation of the *t*Bu group with $\Delta G^{\neq} = 9.3\ \mathrm{kcal\,mol^{-1}}$.[23] In the case of binding of a *t*Bu group to an SWNT, the steric hindrance is even more pronounced, because the C atoms of nanotubes are considerably less pyramidalized[3] and this increases the repulsive interaction between the very bulky binding partners. We have recently provided experimental evidence for this hindrance by demonstrating, by STM, frozen rotation of the *t*Bu group in $t\mathrm{Bu}_n$-SWNT at low temperatures.[12] It is very interesting that although *t*BuLi is less reactive than *n*BuLi, it is also less selective for the attack of metallic tubes. This cannot be explained by single-step additions of *t*Bu anions to the tubes because when the binding of *t*Bu groups is less favorable, the selectivity should increase. Especially in the case of the reaction with *t*BuLi, which is by far the strongest reducing reagent in this series (with the highest HOMO energy), it is possible that a fast electron transfer to the tube can be a competitive initial process. An electron transfer process is further facilitated by the lower propensity of the *t*Bu group to bind directly to the sidewall of the tubes. The importance of electron transfer preceding covalent binding has been considered for the addition of organometallics to C_{60}, and was confirmed for amine additions to fullerenes.[5] In the reaction of diazonium salts with SWNTs also, electron transfer (in this case from the tube to the addend) was suggested to be the initial process.[10] The next step in the formation of the intermediates R_n-SWNT^{n-} would be the considerably slower nucleophilic addition of *t*BuLi present in large excess. This is now less favorable because of electrostatic repulsion. At the same time reactions with nonreduced semiconducting tubes become more preferred because no electrostatic repulsion has to be overcome.

Besides Raman spectroscopy, NIR fluorescence spectroscopy represents another very powerful technique for the specific characterization of SWNTs. In this paper we present this method for the first time in detail for the investigation of sidewall-functionalized nanotubes. The detection of the near-IR photoluminescence across the band gap in semiconducting tubes can be achieved only in isolated SWNTs; otherwise neighboring metallic nanotubes in the bundles would quench the fluorescence.[24] This exfoliation was accomplished by using sodium dodecylbenzenesulfonate (SDBS) as a surfactant in water.[25] Solutions with a concentration of 0.1 mg SWNTs per mL water/SDBS solution were prepared and samples were taken from the supernatant after sonication and precipitation of the insoluble nanotubes. All the functionalized samples exhibited lower fluorescence intensities than the starting material, as a result of two different effects: 1) the decreased solubility of the samples in water/SDBS with higher degrees of functionalization (according to the Raman results); 2) a limited fluorescence quantum efficiency by fast nonradiative decay channels, which may be associated with trapping at defect sites.[26] We used a Kataura plot,[27] based on empirical results of spectrofluorimetric data for identified SWNTs in aqueous SDS suspension and

fitted to empirical expressions, to assign the observed S_{11} bands to nanotube chirality indices and diameters. It is reported that only small systematic spectral shifts of less than 2% can be expected for individual SWNTs suspended in other aqueous surfactants.[26,28] In typical fluorescence spectra of the pristine HiPco material (Figure 6, solid line) at excitation wavelengths of 660 and 785 nm. The bands at 954, 978, 1026, 1058, 1110, 1124, 1175, 1199, 1250, 1323, and 1371 nm are attributed to the indices (8,3), (6,5), (7,5), (10,2), (8,4), (7,6), (8,6), (11,3), (10,3) and/or (10,5), (9,7), and (11,4), with diameters of 0.78, 0.76, 0.83, 0.88, 0.84, 0.90, 0.97, 1.01, 0.94 and/or 1.05, 1.10, and 1.07 nm respectively.[21]

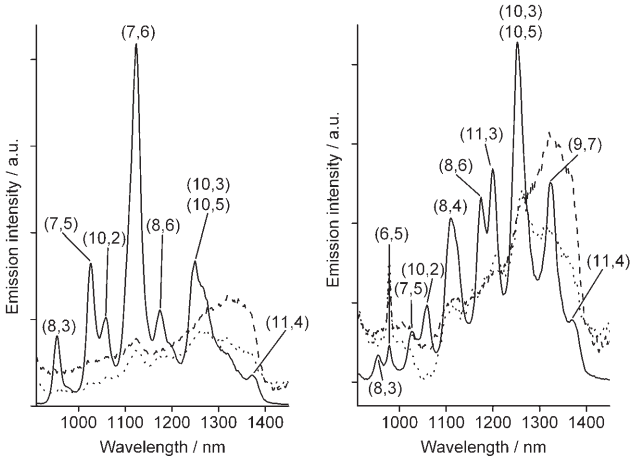

Figure 6. Fluorescence spectra (left: 660 nm excitation, right: 785 nm excitation) of pristine SWNTs (solid line), nBu$_n$(Li)-SWNTs (broken line), and tBu$_n$(Li)-SWNTs (dotted line). For better comparison the relative peak intensities in the spectra of the pristine tubes were reduced by a factor of 10.

In the fluorescence spectra of nBu$_n$(Li)- and tBu$_n$(Li)-SWNTs (also shown in Figure 6), the emission intensities of the functionalized samples are much lower and the bands are broadened significantly compared to the pristine material. To provide better comparability the spectra of the pristine material were reduced in emission intensity by a factor of 10. UV/Vis–NIR absorption spectra (Figure 7) of the same samples in D_2O/SDBS corroborate these results and demonstrate the typical loss of the absorption features associated with covalent sidewall functionalization.[11a] The disappearance of the features in the region of the M_{11} transitions ($\approx$400–600 nm) of the metallic tubes, in comparison to the pristine material, is significant.[11a] The fluorescence results are in good agreement with the Raman investigation in the semiconducting regime (780 nm excitation). Increasing the degree of functionalization of the semiconducting tubes causes a reduction of (Raman) emission intensity. nBu$_n$(Li)-SWNT exhibit higher emission intensity than tBu$_n$(Li)-SWNT tubes. The preferred reaction of the small-diameter tubes is also clear. At the excitation wavelength of 660 nm the intensities of the peaks caused by the (8,3), (7,5), (10,2), and (7,6) tubes are strongly reduced compared to those of the (8,6), (10,3)/(10,5), and (11,4) tubes. Excitation at 785 nm reveals the same trend, with two exceptions. The peak at 978 nm ((6,5) tube) with the smallest diameter (0.76 nm) in this series of (not detectable at 660 nm excitation) is very sharp and intense. This sharp peak is also found in the corresponding spectra of the functionalized tubes R$_n$-SWNT (Figure 8). One explanation is that the (6,5) tube has

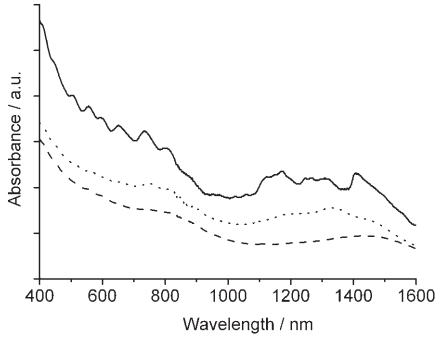

Figure 7. UV/Vis–NIR spectra of pristine SWNTs (solid line), nBu$_n$(Li)-SWNTs (broken line), and tBu$_n$(Li)-SWNTs (dotted line).

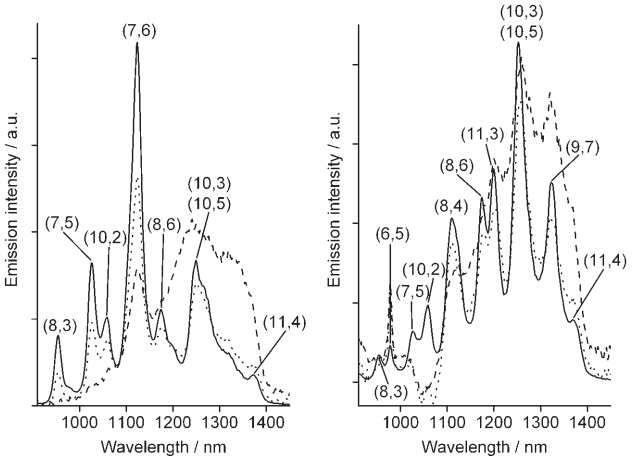

Figure 8. Fluorescence spectra (left: 660 nm excitation, right: 785 nm excitation) of pristine SWNTs (solid line), nBu$_n$(Mg)-SWNTs (broken line), and tBu$_n$(Mg)-SWNTs (dotted line). The intensity of the pristine SWNTs is decreased by a factor of 10.

almost not been functionalized at all, another that this tube species has a particularly high solubility in SDBS/water at low degrees of functionalization. Fluorescence spectroscopy of individualized SWNTs is a very sensitive method and shows some changes, which are not observable by Raman spectroscopy of the bulk material, in greater detail. Illustrative examples are the spectra of nBu$_n$(Mg)- and tBu$_n$(Mg)-SWNTs (Figure 8). The Raman spectra taken in the semiconducting regime (780 nm; Figure 5) displayed only very small changes in the RMB region and, especially for tBu$_n$(Mg)-SWNT, no changes of the D band can be observed. In contrast the corresponding fluorescence spectra clearly reveal the preferred alkylation of the smaller-diame-

ter tubes with the chirality indices (8,3), (7,5), (10,2), (8,4), and (7,6), which exhibit considerably lower intensity than those of the higher-diameter tubes with the chirality indices (8,6), (11,3), (10,3)/(10,5), (9,7), and (11,4). This behavior is less pronounced for $t\mathrm{Bu}_n(Mg)$-SWNT, for which the peaks are sharper, almost like the pristine material, but the emission intensity is still strongly decreased compared to the starting material (the spectra of the functionalized tubes in Figure 8 are magnified by a factor of 10 for better comparison). This corroborates the results obtained by Raman spectroscopy (Figures 4 and 5) and clearly demonstrates that the reaction with *t*BuMgCl leads to the lowest degrees of functionalization in this series. Here, only fluorescence spectroscopy is sensitive enough to detect the changes caused by the sidewall functionalization. The fluorescence spectra of $\mathrm{Et}_n(Li)$-SWNT and $n\mathrm{Hex}_n(Li)$-SWNT are comparable to those of $n\mathrm{Bu}_n(Li)$- and $t\mathrm{Bu}_n(Li)$-SWNTs.

Conclusion

The reaction of SWNTs with organolithium and magnesium compounds exhibits pronounced selectivity. In general, metallic tubes are more reactive than semiconducting ones. This is explained by the finite density of states above the Fermi level in metallic tubes. The reactivity of SWNTs toward the addition of organometallic compounds is inversely proportional to the diameter: for example, tubes with a smaller diameter and more highly pyramidalized sp^2 C atoms are more reactive. This is a result of higher strain energy, which can be relieved after sidewall addition. Previous theoretical calculations clearly predicted this trend.[3] We find diameter selectivity both for metallic and semiconducting tubes. The reactivity depends also on the steric demands of the addend. Binding of the bulky *t*-butyl addend is less favorable than the addition of primary alkyl groups. Significantly, although *t*BuLi is less reactive than, for example, *n*BuLi, it is less selective toward the preferred reaction with metallic tubes. The explanation for this unexpected behavior is that fast electron transfer to the metallic SWNTs, which have low lying electronic states close to the Fermi level, represents a competitive initial process. This is especially important for *t*BuLi, as it has by far the highest HOMO energy and lowest oxidation potential in this series of reagents. An electron-transfer process is further facilitated by the lower propensity, as a result of steric hindrance, of the *t*Bu group to bind directly to the sidewalls of the tubes. The subsequent addition of *t*BuLi to reduced metallic tubes is then disfavored, as a result of electrostatic repulsion. The latter finding implies that the reactivity and selectivity of SWNTs toward the reaction with organometallic compounds can be influenced further by preceding reduction or oxidation steps. Initial chemical or electrochemical reduction should decrease the reactivity of metallic tubes, and oxidation should increase it. After highly efficient and selective sidewall binding of the addends, the increased solubility of functionalized metallic SWNTs should enable separation from unreacted semiconducting tubes by extraction. We have shown previously that the electronic properties of the parent SWNTs can be recovered after thermal cleavage of the addends.[12] Highly efficient separation of metallic from semiconducting tubes is still a challenge.[11] Even more challenging is the separation according to the difference in tube diameter.[7–10] Work along these lines based on the findings presented in this study is currently under way in our laboratory. We have also reported for the first time on the NIR emission of weakly functionalized semiconducting SWNTs. Our findings imply interesting applications of functionalized tubes as novel fluorescent reporter molecules in, for example, biological systems, which has already proven to be a successful concept in the case of noncovalently modified SWNTs.[22a,29]

Experimental Section

General: SWNTs were obtained from Carbon Nanotechnologies Inc. (purified HiPco® single-wall carbon nanotubes) and further purified by sonication and boiling in hydrochloric acid (37%). Chemicals and solvents were purchased from Acros (Geel, Belgium) and used as received. Raman spectra were recorded from the solid (bucky paper) with a Thermo Nicolet Almega XR dispersive Raman spectrometer ($\lambda_{ex}=532$ and 780 nm). Fluorescence spectra were recorded with an NS1 NanoSpectralyzer from Applied NanoFluorescence LLC ($\lambda_{ex}=660$ and 785 nm) in a solution of sodium dodecylbenzenesulfonate (SDBS, 1% w/w) in water (0.1 mg SWNTs per mL). The spectra were measured from the supernatant after sonication (5 min) and precipitation (one day) of the insoluble SWNTs. Samples for UV/Vis-NIR measurement were prepared analogously but in D_2O instead of water. The spectra were recorded with a Shimadzu UV3102-PC instrument. Thermogravimetric analysis with mass spectroscopy (TGA-MS) was accomplished on a Netzsch STA 409 CD instrument with Skimmer QMS 422 (temperature program: 80°C for 30 min, 80–600°C with a 10°C min^{-1} gradient and 600°C for 30 min; initial weights ≈5–10 mg. Sonications were performed with a Bandelin Sonorex RK 106 or with a Hielscher UP400S ultrasonic processor.

General procedure for synthesis of $\mathrm{R}_n(M)$-SWNT: In a nitrogen-purged and heat-dried four-necked round-bottomed flask (250 mL), equipped with two gas inlets and pressure compensation, purified HiPCO SWNTs (20 mg, 1.7 mmol of carbon) were dispersed in anhydrous cyclohexane (100 mL) under sonication (15 min). To this dispersion ethyllithium (1.7 M in butyl ether), *n*-butyllithium (1.6 M in hexane), *t*-butyllithium (1.5 M in pentane), *n*-hexyllithium (2.3 M in hexane), *n*-butylmagnesium chloride (1.7 M in THF/toluene), or *t*-butylmagnesium chloride (1.7 M in THF) in fivefold excess (related to moles of carbon) was added dropwise over a 10 min period. The resulting suspension was then stirred (30 min, RT or 0°C) and subsequently sonicated (30 min), resulting in a stable, black, homogeneous dispersion. The reaction mixture was stirred (20 h, RT or 0°C) and successively quenched by bubbling oxygen through the solution (30 min). The heterogeneous dispersion formed was diluted with cyclohexane (100 mL), transferred into a separation funnel, and purged with water and dilute hydrochloric acid until the pH value remained neutral. The organic layer with the nanotubes was filtered through a PP membrane filter (0.2 μm) and washed with cyclohexane, ethanol, and water. The resulting black solid was dried in a vacuum oven (50°C) overnight to produce a bucky paper of $\mathrm{R}_n(M)$-SWNTs.

Acknowledgement

This work was supported by the Deutsche Forschungsgemeinschaft (DFG).

[1] See, for example: a) *The Science and Technology of Carbon Nanotubes* (Eds.: K. Tanaka, T. Yamabe, K. Fukui), Elsevier, Oxford, **1999**; b) *Carbon Nanotubes: Synthesis, Structure, Properties and Applications* (Eds.: P. Avouris, G. Dresselhaus, M. S. Dresselhaus), Springer-Verlag, Berlin, **2000**; c) *Applied Physics of Carbon Nanotubes* (Eds.: S. V. Rotkin, S. Subramoney), Springer-Verlag, Berlin, **2005**.

[2] See, for example: a) A. Hirsch, *Angew. Chem.* **2002**, *114*, 1933–1939; *Angew. Chem. Int. Ed.* **2002**, *41*, 1853–1859; b) O. Vostrowsky, A. Hirsch, *Angew. Chem.* **2004**, *116*, 2380–2383; *Angew. Chem. Int. Ed.* **2004**, *43*, 2326–2329; c) C. A. Dyke, J. M. Tour, *J. Phys. Chem. B* **2004**, *108*, 11151–11159; d) K. Balasubramanian, M. Burghard, *Small* **2005**, *1*, 180–192; e) S. Banerjee, T. Hemraj-Benny, S. S. Wong, *Adv. Mater.* **2005**, *17*, 17–29; f) A. Hirsch, O. Vostrowsky, *Top. Curr. Chem.* **2005**, *245*, 193–237; g) D. Tasis, N. Tagmatarchis, A. Bianco, M. Prato, *Chem. Rev.* **2006**, *106*, 1105–1136.

[3] Z. Chen, W. Thiel, A. Hirsch, *ChemPhysChem* **2003**, *4*, 93–97.

[4] a) J. L. Bahr, J. M. Tour, *J. Mater. Chem.* **2002**, *12*, 1952–1958; b) X. Lu, F. Tian, X. Xu, N. Wang, Q. Zhang, *J. Am. Chem. Soc.* **2003**, *125*, 10459–10464; c) K. Seo, K. A. Park, C. Kim, S. Han, B. Kim, Y. H. Lee, *J. Am. Chem. Soc.* **2005**, *127*, 15724–15729.

[5] *Fullerenes: Chemistry and Reactions* (Eds.: A. Hirsch, M. Brettreich), Wiley-VCH, Weinheim, **2005**.

[6] a) H. Hayden, Y. K. Gun'ko, T. S. Perova, *Chem. Phys. Lett.* **2007**, *435*, 84–89; b) L. Zhang, J. Yang. C. L. Edwards, L. B. Alemany, V. N. Khabashesku, A. R. Barron, *Chem. Commun.* **2005**, 3265–3267; c) J. L. Delgado, P. de la Cruz, F. Langa, A. Urbina, J. Casado, J. T. López Navarrete, *Chem. Commun.* **2004**, 1734–1735.

[7] W. Zhou, Y. H. Ooi, R. Russo, P. Papanek, D. E. Luzzi, J. E. Fischer, M. J. Bronikowski, P. A. Willis, R. E. Smalley, *Chem. Phys. Lett.* **2001**, *350*, 6–14.

[8] G. Zhang, D. Mann, L. Zhang, A. Javey, Y. Li, E. Yenilmez, Q. Wang, J. P. McVittie, Y. Nishi, J. Gibbons, H. Dai, *Proc. Natl. Acad. Sci. USA* **2005**, *102*, 16141–16145.

[9] S. Banerjee, S. S. Wong, *Nano Lett.* **2004**, *4*, 1445–1450.

[10] N. Nair, W.-J. Kim, M. L. Usrey, M. S. Strano, *J. Am. Chem. Soc.* ***2007***, *129*, 3946–3954.

[11] a) M. S. Strano, C. A. Dyke, M. L. Usrey, P. W. Barone, M. J. Allen, H. Shan, C. Kittrell, R. H. Hauge, J. M. Tour, R. E. Smalley, *Science* **2003**, *301*, 1519–1522; b) M. S. Strano, *J. Am. Chem. Soc.* **2003**, *125*, 16148–16153; c) K. H. An, J. S. Park, C.-M. Yang, S. Y. Jeong, S. C. Lim, C. Kang, J.-H. Son, M. S. Jeong, Y. H. Lee, *J. Am. Chem. Soc.* **2005**, *127*, 5196–5203; d) S. Toyoda, Y. Yamaguchi, M. Hiwatshi, Y. Tomonari, H. Muratami, N. Nakashima, *Chem. Asian J.* **2007**, *2*, 145–149.

[12] R. Graupner, J. Abraham, D. Wunderlich, A. Vencelova, P. Lauffer, J. Röhrl, M. Hundhausen, L. Ley, A. Hirsch, *J. Am. Chem. Soc.* **2006**, *128*, 6683–6689.

[13] a) F. Liang, A. K. Sadana, A. Peera, J. Chattopadhyay, Z. Gu, R. H. Hauge, W. E. Billups, *Nano Lett.* **2004**, *4*, 1257–1260; b) F. Liang, L. B. Alemany, J. M. Beach, W. E. Billups, *J. Am. Chem. Soc.* **2005**, *127*, 13941–13948; c) J. Chattopadhyay, A. K. Sadana, F. Liang, J. M. Beach, Y. Xiao, W. E. Billups, *Org. Lett.* **2005**, *7*, 4067–4069.

[14] E. Joselevich, *ChemPhysChem* **2004**, *5*, 619–624.

[15] P. Nikolaev, M. J. Bronikowski, R. K. Bradley, F. Rohmund, D. T. Colbert, K. A. Smith, R. E. Smalley, *Chem. Phys. Lett.* **1999**, *313*, 91–97.

[16] S. Chen, W. Shen, G. Wu, D. Chen, M. Jiang, M. Jiang, *Chem. Phys. Lett.* **2005**, *402*, 312–317.

[17] See for example: a) M. S. Dresselhaus, G. Dresselhaus, A. Jorio, A. G. Souza Filho, M. A. Pimenta, R. Saito, *Acc. Chem. Res.* **2002**, *35*, 1070–1078; b) M. S. Dresselhaus, G. Dresselhaus, R. Saito, A. Jorio, *Phys. Rep.* **2005**, *409*, 47–99.

[18] M. Burghard, *Surf. Sci. Rep.* **2005**, *58*, 1–109.

[19] a) A. Mews, C. Y. Jiang, T. Schuessler, G. Philipp, Y. Fan, M. Burghard, *Isr. J. Chem.* **2001**, *41*, 15–22; b) P. R. Marcoux, J. Schreiber, P. Batail, S. Lefrant, J. Renouard, G. Jacob, D. Albertini, Y. Y. Mevellec, *Phys. Chem. Chem. Phys.* **2002**, *4*, 2278–2285.

[20] a) H. Kataura, Y. Kumazawa, Y. Maniwa, I. Umezu, S. Suzuki, Y. Ohtsuka, Y. Achiba, *Synth. Met.* **1999**, *103*, 2555–2558; b) M. Hulman, R. Pfeiffer, H. Kuzmany, *New J. Phys.* **2004**, *6*, 1–17; c) H. Telg, J. Maultzsch, S. Reich, F. Hennrich, C. Thomsen, *Phys. Rev. Lett.* **2004**, *93*, 177401; d) A. Jorio, C. Fantini, M. A. Pimenta, R. B. Capaz, G. G. Samsonidze, G. Dresselhaus, M. S. Dresselhaus, J. Jiang, N. Kobayashi, R. Saito, *Phys. Rev. B* **2005**, *71*, 075401.

[21] A. Kukuvecz, T. Pichler, R. Pfeiffer, C. Kramberger, H. Kuzmany, *Phys. Chem. Chem. Phys.* **2003**, *5*, 582–587.

[22] a) S. M. Bachilo, M. S. Strano, C. Kittrell, R. H. Hauge, R. E. Smalley, R. B. Weisman, *Science* ***2002***, *298*, 2361–2366; b) A. Kukovecz, C. Kramberger, V. Georgakilas, M. Prato, H. Kuzmany, *Eur. Phys. J. B* **2002**, *28*, 223–230; c) V. C. Moore, M. S. Strano, E. H. Haroz, R. H. Hauge, R. E. Smalley, J. Schmidt, Y. Talmon, *Nano Lett.* **2003**, *3*, 1379–1382.

[23] P. J. Fagan, P. J. Krusic, D. H. Evans, S. A. Lerke, E. Johnston, *J. Am. Chem. Soc.* **1992**, *114*, 9697–9699.

[24] M. J. O'Connell, S. M. Bachilo, C. B. Huffman, V. C. Moore, M. S. Strano, E. H. Haroz, K. L. Rialon, P. J. Boul, W. H. Noon, C. Kittrell, J. Ma, R. H. Hauge, R. B. Weisman, R. E. Smalley, *Science* **2002**, *297*, 593–596.

[25] a) C. A. Dyke, J. M. Tour, *Nano Lett.* **2003**, *3*, 1215–1218; b) V. C. Moore, M. S. Strano, E. H. Haroz, R. H. Hauge, R. E. Smalley, J. Schmidt, Y. Talmon, *Nano Lett.* **2003**, *3*, 1379–1382.

[26] F. Wang, G. Dukovic, L. E. Brus, T. F. Heinz, *Phys. Rev. Lett.* **2004**, *92*, 177401.

[27] R. B. Weisman, S. M. Bachilo, *Nano Lett.* **2003**, *3*, 1235–1238.

[28] S. Lebedkin, F. H. Hennrich, T. Skipa, M. M. Kappes, *J. Phys. Chem. B* **2003**, *107*, 1949–1956.

[29] P. Cherukuri, C. J. Gannon, T. K. Leeuw, H. K. Schmidt, R. E. Smalley, S. A. Curley, R. B. Weisman, *Proc. Natl. Acad. Sci. USA* **2006**, *103*, 18882–18886.

Received: July 6, 2007
Published online: November 23, 2007

